A path integral study of the role of correlation in exchange coupling of spins in double quantum dots and optical lattices

2010 J. Phys.: Condens. Matter 22 145301

(http://iopscience.iop.org/0953-8984/22/14/145301)

IOP Publishing Journal of Physics: Condensed Matter

J. Phys.: Condens. Matter **22** (2010) 145301 (5pp) doi:10.1088/0953-8984/22/14/145301

A path integral study of the role of correlation in exchange coupling of spins in double quantum dots and optical lattices

Jesper Goor Pedersen[1], **Lei Zhang**[2], **M J Gilbert**[3] **and J Shumway**[2,4]

[1] DTU Fotonik, Technical University of Denmark, Kongens Lyngby, Denmark
[2] Department of Physics, Arizona State University, Tempe, AZ 85287-1504, USA
[3] Department of Electrical and Computer Engineering, University of Illinois, Urbana, IL 61801, USA

E-mail: john.shumway@asu.edu

Received 29 January 2010, in final form 22 February 2010
Published 19 March 2010
Online at stacks.iop.org/JPhysCM/22/145301

Abstract

We explore exchange coupling of a pair of spins in a double dot and in an optical lattice, using the frequency of exchanges in a bosonic path integral, evaluated using Monte Carlo simulation. The algorithm gives insights into the role of correlation through visualization of two-particle probability densities, instantons, and the correlation hole. We map the problem to the Hubbard model and see that exchange and correlation renormalize the model parameters, dramatically reducing the effective on-site repulsion at larger separations.

(Some figures in this article are in colour only in the electronic version)

Lattice models are popular in solid state physics and often serve as simple models for atomic orbitals, especially in the theory of magnetism [1]. Quantum dot arrays and optical lattices are new realizations of lattices. These artificial lattices are candidates for quantum computers, where spins on exchange-coupled dots are qubits for universal quantum computation [2, 3]. A fundamental concept is intersite exchange, in which virtual hopping leads to spin coupling of neighboring sites. A two-site model is one of the simplest quantum problems, yet the quantitative mapping from a three-dimensional model of a double dot or optical lattice experiment to an effective two-site model has many subtleties requiring careful treatment of exchange and correlation [1, 3–6].

In this paper we use path integral Monte Carlo (PIMC) to extract accurate singlet–triplet splitting from a spatial model. Similar PIMC algorithms have been used to study spin dynamics in ^{3}He [7–9] and Wigner crystals [8, 10], and the approach is particularly simple for two-site models. This two-particle problem has been previously solved with direct diagonalization (DD) methods with a careful choice of basis functions [4, 6] and is amenable to variational or diffusion quantum Monte Carlo (QMC) [11]. However, the simple and elegant PIMC approach is a more direct solution without variational bias or basis set issues and offers theoretical insights into this important problem. We first show that the splitting energy, J, is easily extracted from the average permutation of the two-particle path integral, even when $J \ll k_B T$. This PIMC algorithm is a black-box calculator, providing accurate numerical estimates of J for technologically relevant models of dots or optical lattices with arbitrary interactions and confinement potentials. More importantly, PIMC allows us to ask questions about quantum correlation. For example, do the particles exchange across the barrier simultaneously, or do they briefly double occupy the dot? Or, does the motion of one particle over the barrier correlate with the location of the other particle? We answer these questions by viewing representative trajectories (instantons) for a double dot and calculating pair correlation functions. Magnetic fields are known to modulate J [3, 4, 6], and we show how to include them in PIMC with a simple Berry's phase [12]. Finally we model recent experiments of exchange coupled atoms in an optical trap, demonstrating broader utility [13].

The mapping from a continuous model with interacting particles to a lattice model introduces subtle complications. For a non-interacting system it is reasonable to reduce the Hilbert space to just one orbital per site, coupled by a hopping matrix element, t. The non-interacting many-body ground

[4] http://shumway.physics.asu.edu.

state is a product state of these single-particle orbitals. Low energy excited states are spanned by this basis, so an effective lattice model is an excellent approximation. Interactions are typically added to this lattice model as on-site energies, U, or intersite terms, V. For small t, this gives the well-known $J = 4t^2/(U - V)$.

There can be a serious flaw when considering interactions in this order. When interactions are added to the continuum Hamiltonian, correlation enters as virtual excitations to higher energy orbitals. At first this seems insignificant, since there may be still a one-to-one mapping to an effective lattice model. But, when choosing effective lattice parameters, one must remember that many-body states in the continuum model have quantum fluctuations that are simply not present in the lattice model.

As a specific example, consider two electrons in a double quantum dot. This system is often represented as a two-site Hubbard model, where the sites represent the 1s ground states of the dots. Correlation terms involve virtual excitation of the electron to the $2p_x$ and $2p_y$ states of the dots. These quantum fluctuations create van der Waals attraction, in addition to mean-field repulsion. Van der Waals attraction and other correlations renormalize the interaction parameters to new values, U_r and V_r.

When we consider hopping between sites, more complications emerge. The hopping barrier has contributions from both the external potential and electron–electron interactions. While the mean-field Hartree contribution can simply be added to the effective potential, the fluctuating part is not so trivial. In the transition state, an electron passes over a barrier whose height has quantum fluctuations. Thus we expect interactions to renormalize the hopping constant, t_r. At the Hartree–Fock level, Hund–Mulliken theory already predicts a renormalized t_r and U_r due to long-range exchange [1, 3]. However, neglect of correlation in Hund–Mulliken theory can lead to catastrophic failure at intermediate dot separations [6]. PIMC includes all correlations, and illuminates their role in barrier hopping with the concept of instantons.

We start with the two-dimensional model for the GaAs double quantum dot studied in [6],

$$H = \frac{\mathbf{p}_1^2}{2m^*} + \frac{\mathbf{p}_2^2}{2m^*} + \frac{e^2}{\epsilon|\mathbf{r}_1 - \mathbf{r}_2|} + V_{\text{ext}}(\mathbf{r}_1) + V_{\text{ext}}(\mathbf{r}_2), \quad (1)$$

with $m^* = 0.067m_e$ and $\epsilon = 12.9$. The external potential comes from two piecewise-connected parabolic potentials,

$$V_{\text{ext}}(\mathbf{r}) = \tfrac{1}{2}m\omega_0\{\min[(x-d)^2, (x+d)^2] + y^2\}, \quad (2)$$

with minima at $x = \pm d$. We report d relative to the oscillator length $r_0 = \sqrt{\hbar/m\omega_0}$. The two lowest energy two-electron states are spatially symmetric and antisymmetric under exchange, with energies ε_+ and ε_-, respectively. The exchange coupling, $J = \varepsilon_- - \varepsilon_+$, has been calculated previously using DD on a basis of Fock states built from seven single particles states [6]. Much care was taken to test convergence with the number of states and careful evaluation of Coulomb matrix elements. We note that the same quality of DD calculation in three dimensions would typically take more single-particle states.

QMC techniques give essentially exact answers to many problems without basis set convergence issues, and often work just as easily in multiple dimensions. PIMC is nice for quantum dot problems [14] because it does not require a trial wavefunction. However, direct calculation of either ε_+ or ε_- with PIMC often have large statistical errors in energy ($\sim$1 meV in dots). Instead, we use particle exchange statistics to estimate energy differences J to high accuracy ($\sim 1\ \mu$eV) in PIMC.

To calculate J, we split the partition function into terms that are spatially symmetric and antisymmetric under exchange, $Z = Z_+ + Z_-$. These terms can be expressed as symmetrized or antisymmetrized imaginary time path integrals [15, 16], (see appendix),

$$Z_\pm = \tfrac{1}{2!}\sum_{P=\mathcal{I},\mathcal{P}} (\pm 1)^P \int \mathcal{D}R(\tau) \mathrm{e}^{-\frac{1}{\hbar}S_{\mathrm{E}}[R(\tau)]}. \quad (3)$$

This is a sum over all two-particle paths $R(\tau)$ with the boundary condition $R(\beta\hbar) = PR(0)$, $(P = \mathcal{I}, \mathcal{P})$, where $\mathcal{P}$ swaps particle positions and $\mathcal{I}$ is the identity. The symbol $(\pm 1)^P$ takes the values $(\pm 1)^{\mathcal{I}} = 1$ and $(\pm 1)^{\mathcal{P}} = \pm 1$. At low temperature, only one state contributes to each partition function, so $Z_\pm = \mathrm{e}^{-\beta\varepsilon_\pm}$. Thus,

$$\mathrm{e}^{-\beta J} = \frac{Z_-}{Z_+} = \frac{\sum_P \int \mathcal{D}R(-1)^P \mathrm{e}^{-\frac{S_{\mathrm{E}}}{\hbar}}}{\sum_P \int \mathcal{D}R \mathrm{e}^{-\frac{S_{\mathrm{E}}}{\hbar}}} \equiv \langle(-1)^P\rangle_+, \quad (4)$$

or $J = -k_{\mathrm{B}}T \ln\langle(-1)^P\rangle_+$. Thus the exchange coupling can be calculated by sampling a symmetric (bosonic) path integral [16] and taking the average of $(-1)^P$, which is $+1$ for identity paths and -1 for exchanging paths.

We ran PIMC simulations [16] with our open-source `pi` code for the dots studied in [6], with the results shown in figure 1(a). To aid other researchers, we have made the simulation available as a tool on nanoHUB [17]. Coulomb interactions are included with a pair action that correctly handles the cusp condition. We observed convergence of the path integral results with 6400 discrete slices, but a higher-quality pair action [16] could require fewer slices. We see near perfect agreement with DD, and speculate that small deviations may be due to the finite basis in the DD calculation or approximations in the evaluation of Coulomb matrix elements at larger d [6].

To learn more, we collect the two-particle density, $\rho(x_1, x_2)$, which is the probability to find one electron at x_1 and the other at x_2, integrated over all values of y_1 and y_2, and shown in figure 2(b). We calculate double occupation, x_{D}, which we define as the probability for the electrons to lie on the same side of the $x = 0$ plane. From J and x_{D} we deduce renormalized values for t_r and $U_r - V_r$, figures 1(c) and (d). Interactions renormalize t_r to smaller values, consistent with Hund–Mulliken theory or a larger renormalized mass. The larger J arises from the dramatic decrease in $U_r - V_r$ at larger dot separations, as correlation enables more virtual hopping.

There are two minima, $(x_1, x_2) = (\pm d, \mp d)$, in the total potential, marked '+' in figure 2(b). For non-zero J, some paths must go between these minima. In a semiclassical

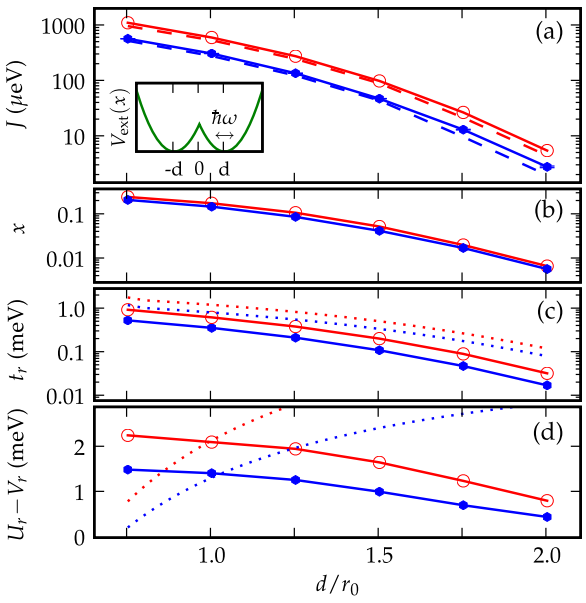

Figure 1. PIMC results. (a) Exchange couplings J for $\hbar\omega = 4$ meV (●) and $\hbar\omega = 6$ meV (○) double dots with a piecewise parabolic potential (inset). Dashed lines are direct diagonalization results from [6]. (b) The double dot occupation probability x. Using J and x we fit (c) t_r and (d) $U_r - V_r$ parameters for an effective two-site Hubbard model. Dashed lines in (c) show the bare hopping t for one electron in the double dot. Dashed lines in (d) are $V - U$ with $V = e^2/2\epsilon d$ and U taken from a PIMC calculation on a single dot.

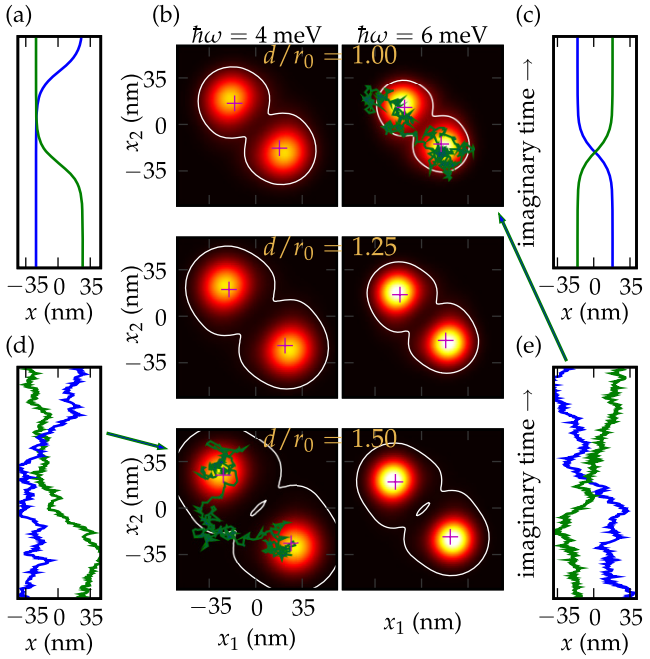

Figure 2. Paths and pair densities for a double dot. (a) Simplified instanton with double occupation of the right dot. (b) Pair densities $\rho(x_1, x_2)$ with the lowest density contour line that connects both potential minima (+ markers) at $(\pm d, \mp d)$. (c) Simplified instanton with simultaneous exchange. (d) Actual path showing double occupation, sampled from $\hbar\omega = 4$ meV, $d = 1.5r_0$ dots. (e) Actual path showing simultaneous exchange, sampled from $\hbar\omega = 6$ meV, $d = r_0$ dots. Trajectories (d) and (e) are also plotted in (b).

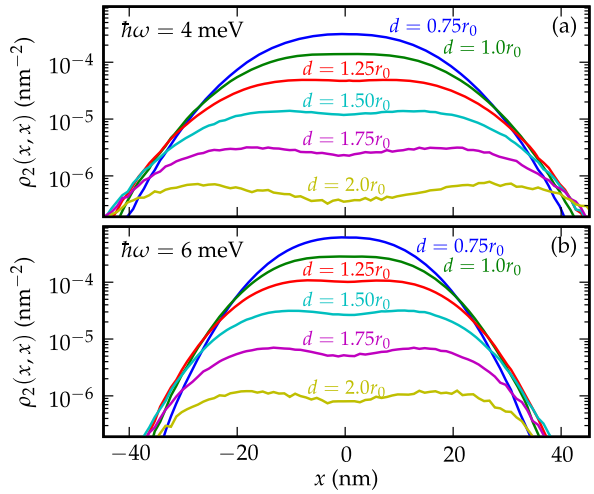

Figure 3. Crossing density, $\rho_2(x, x)$, equivalent to the diagonal of the pair densities in figure 2(b).

picture, the paths fluctuate around the potential minima, with rapid crossings called instantons, in which particles exchange between the dots. An instanton can involve brief double occupation of a dot, illustrated in figure 2(a), or simultaneous exchange, as in figure 2(c). Figures 2(d) and (e) show paths from PIMC that resemble the idealized instantons. In figure 2(b), one instanton moves from the $(d, -d)$ minimum, briefly double occupies the left dot, $(-d, -d)$, then moves to the $(-d, d)$ minimum, while the other instanton moves directly between the two minima.

Contours of $\rho(x_1, x_2)$, figure 2(b), reveal a trend with increasing dot separation. For small d the highest probability is directly between the minima (simultaneous exchange), but at larger d the highest probability has two pathways (brief double occupation). Figure 3 shows the probability density for crossing, $\rho(x, x)$. Crossing is most likely in the middle ($x = 0$) when the dots are close together. For larger d, the crossing probability has a double peak near the dots that is about twice the value at $x = 0$. The double peaks are slightly larger for the wider $\hbar\omega = 4$ meV dot, indicating more double occupation.

To underscore the presence of electronic correlation during tunneling, we plot the correlation hole in figure 4, with PIMC results next to DD results [6]. While some quantitative differences are apparent, consistent with the finite basis size in DD, the overall agreement is quite good. The message is clear: in the instanton, as one electron moves between the dots, the other electron moves away, enhancing the instanton and increasing J.

For charged particles, magnetic fields can be used to tune the exchange coupling and even change its sign [3, 18]. In the path integral, a magnetic field is easily implemented as a Berry's phase $q\Phi_B$, where q is the electron charge and Φ_B is the total magnetic flux enclosed by the path of the two electrons. The exchange splitting is then $J(B) = -k_B T \ln(\langle e^{iq\Phi_B}(-1)^P\rangle_+ / \langle e^{iq\Phi_B}\rangle_+)$. The quantities are averaged from the bosonic path integral with no field, so data for different B-fields may be collected simultaneously. For very large magnetic fields the expectation value in the

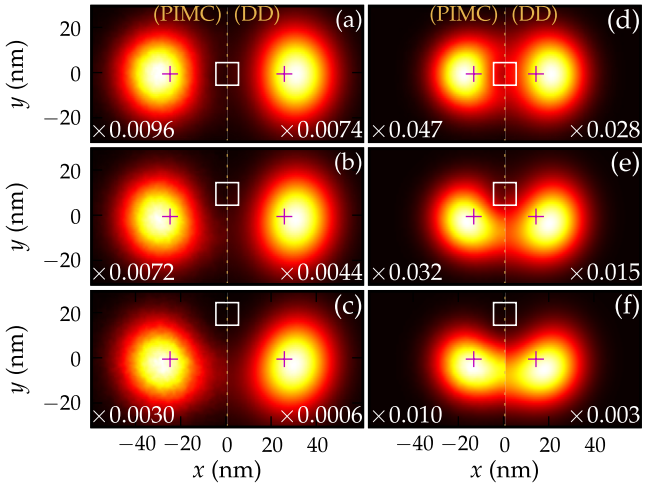

Figure 4. Conditional density of one electron when the other electron is in the white box, showing the correlation hole during an instanton. Panels (a)–(c) are the $\hbar\omega = 4$ meV, $d = 1.5r_0$ dots and (d)–(f) are the $\hbar\omega = 6$ meV, $d = 1.0r_0$ dots. Numerical factors are the likelihood of the first electron being in the white box. PIMC results are shown on the left of each image, with DD results [6] on the right.

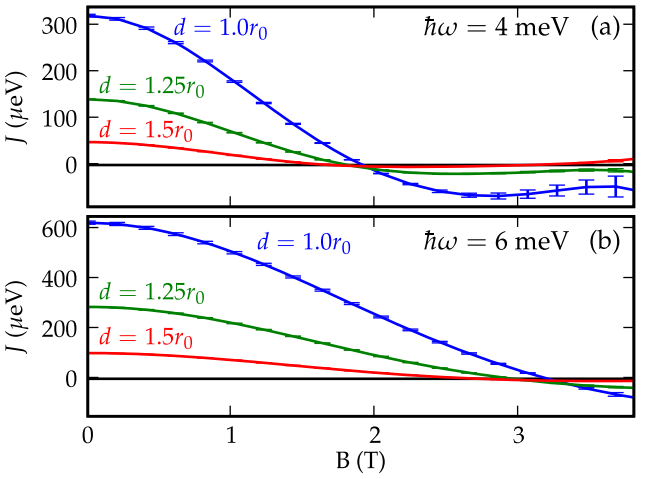

Figure 5. Magnetic field dependence included with a Berry's phase for several double quantum dots.

denominator is small and Monte Carlo sampling errors are catastrophic. In practice, we find that fields up to 4 T in strength are practical for the geometries we study, yielding the results in figure 5.

To test the applicability of the method to an optical lattice, we consider the exchange of two ^{87}Rb atoms in a double-well optical trap [13]. This system resembles the double dot, only with much heavier particles, a much lower temperature, short-range interactions, and a different confining potential. While the experiments in [13] have very little correlation, we present results to demonstrate feasibility for such systems, which can be made more strongly interacting. The experiment has a double-well potential, $V(x) = V_{\text{long}} \sin^2(\pi x/\lambda) + V_{\text{short}} \cos^2(2\pi x/\lambda)$, with $\lambda = 765$ nm and $V_{\text{long}} = 10E_{\text{r}}$, where $E_{\text{r}} = h^2/2M_{\text{Rb}}\lambda^2$ [13]. We model interactions as $V(r) = V_0 \text{sech}^2 \kappa r$ with $V_0 = 50.5\ \mu$K and $\kappa = 0.1$ nm^{-1} to

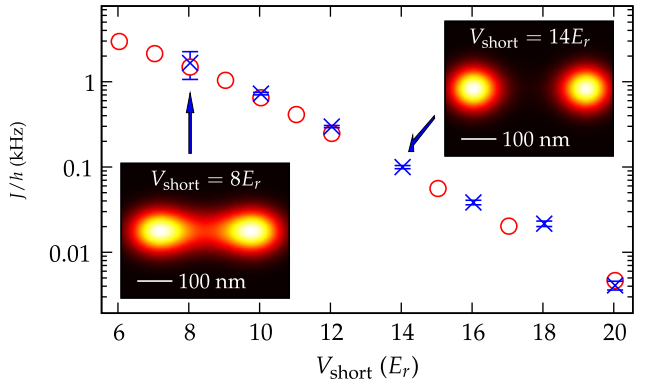

Figure 6. Spin splitting of ^{87}Rb atoms trapped in a double well: ×, PIMC results at 10 nK, and ○, experimental data [13]. Insets show atomic probability densities.

reproduce the ^{87}Rb scattering length. Figure 6 shows J as the barrier V_{short} is varied, confirming agreement with experiment.

In conclusion, we have demonstrated a PIMC algorithm for computing exchange splitting in double quantum dots and optical lattices. The exchange splitting arises from instantons in the path integral, and we have collected data on these path crossings, including double occupation and the correlation hole. Correlations renormalize t_{r} and $U_{\text{r}} - V_{\text{r}}$, with a dramatic decrease in $U_{\text{r}} - V_{\text{r}}$ at large separation. We find that simultaneous crossing occurs more often with closely spaced dots, while further separated dots are more likely to have instantons with double occupations. Finally, we have demonstrated the versatility of the algorithm with the inclusion of magnetic fields and applications to laser-trapped atoms.

Acknowledgments

Work supported by NSF Grant No. DMR 0239819 and NRI-SWAN and made use of facilities provided by the Ira A Fulton High Performance Computing Initiative. JS thanks Erich Mueller for helpful discussions.

Appendix. Form of the discretized path integral and the action

The partition function for the effective mass Hamiltonian, equation (1), can be written as an imaginary time path integral [14–16],

$$Z = \int \mathcal{D}R(\tau) \mathrm{e}^{-\frac{1}{\hbar} S_{\text{E}}[R(\tau)]}. \tag{A.1}$$

The path integral $\int \mathcal{D}R(\tau)$ and Euclidean action S_{E} are easiest to define in the discretized form we used in the Monte Carlo integration. By dividing imaginary time into N_T discrete steps, each of length $\Delta\tau = \beta\hbar/N_T$, the path $R(\tau)$ becomes an array of positions ('beads') $\mathbf{r}_{ij}$, where i indicates the slice number ($0 \leqslant i < N_T$) and $j = 1, 2$ labels the two electrons. Then the path integral becomes a multiple integral over all bead

positions,

$$\int \mathcal{D}R(\tau) \to \prod_{i=0}^{N_T-1} \int \mathrm{d}\mathbf{r}_{1\,j} \int \mathrm{d}\mathbf{r}_{2\,j}. \tag{A.2}$$

The action S_E represents the terms in the effective mass Hamiltonian and is a function of the bead coordinates,

$$S_\mathrm{E} = \sum_{i=0}^{N_T-1} \Bigg[\frac{m^*|\mathbf{r}_{i+1\,1} - \mathbf{r}_{i\,1}|^2}{2\,\Delta\tau} + \frac{m^*|\mathbf{r}_{i+1\,2} - \mathbf{r}_{i\,2}|^2}{2\,\Delta\tau} + 2\ln(2\pi\,\Delta\tau/m^*) + V_\mathrm{ext}(\mathbf{r}_{i\,1})\Delta\tau + V_\mathrm{ext}(\mathbf{r}_{i\,2})\Delta\tau + u_\mathrm{coul}(\mathbf{r}_{i+1\,1}, \mathbf{r}_{i+1\,2}, \mathbf{r}_{i,1}, \mathbf{r}_{i,2}; \Delta\tau) \Bigg]. \tag{A.3}$$

The first three terms (which explicitly contain m^*) are the kinetic action and are derived from the free particle propagator in two dimensions. The next two terms are the action for the confining potential, $V_\mathrm{ext}(\mathbf{r})$, evaluated in the primitive approximation [16]. The last term is the pair Coulomb action [16], which we have fit to a short time approximation of the Coulomb propagator for the imaginary time interval $\Delta\tau$. Because of special symmetry of the Coulomb potential, this propagator is only a function of two coordinates, $q_i = (|\mathbf{r}_{i+1\,1} - \mathbf{r}_{i+1\,2}| + |\mathbf{r}_{i\,1} - \mathbf{r}_{i\,2}|)/2$ and $s_i^2 = |(\mathbf{r}_{i+1\,1} - \mathbf{r}_{i+1\,2}) - (\mathbf{r}_{i\,1} - \mathbf{r}_{i\,2})|^2$. For simplicity, we have dropped the s^2 dependence; this approximation is exact as $\Delta\tau \to 0$. We evaluated the short time Coulomb propagator using the high-accuracy Trotter method of [19] and stored tabulated values of $u_\mathrm{coul}(q; \Delta\tau)$ on a grid for efficient evaluation during our Monte Carlo simulations.

To perform the trace implicit in equation (A.1), we identify slice N_T with slice 0 in equation (A.3) by setting $\mathbf{r}_{N_T\,1} = \mathbf{r}_{0\,1}$ and $\mathbf{r}_{N_T\,2} = \mathbf{r}_{0\,2}$. The division of the partition function into spatially symmetric Z_+ and antisymmetric Z_- parts may be accomplished by summing over permutations $P = \mathcal{I}, \mathcal{P}$, as in equation (3). Permuting configurations ($P = \mathcal{P}$) are handled by setting $\mathbf{r}_{N_T\,1} = \mathbf{r}_{0\,2}$ and $\mathbf{r}_{N_T\,2} = \mathbf{r}_{0\,1}$ in equation (A.3).

References

[1] Mattis D C 1981 *The Theory of Magnetism* (*Springer Series in Solid-State Science* vol 17) (Berlin: Springer)
[2] Loss D and DiVincenzo D P 1998 *Phys. Rev.* A **57** 120–6
[3] Burkard G, Loss D and DiVincenzo D P 1999 *Phys. Rev.* B **59** 2070–8
[4] Helle M, Harju A and Nieminen R M 2005 *Phys. Rev.* B **72** 205329
[5] Melnikov D V, Leburton J P, Taha A and Sobh N 2006 *Phys. Rev.* B **74** 041309(R)
[6] Pedersen J, Flindt C, Mortensen N A and Jauho A P 2007 *Phys. Rev.* B **76** 125323
[7] Thouless D J 1965 *Proc. Phys. Soc.* **86** 893–904
[8] Roger M 1984 *Phys. Rev.* B **30** 6432–57
[9] Ceperley D M and Jacucci G 1987 *Phys. Rev. Lett.* **58** 1648–51
[10] Bernu B, Cândido L and Ceperley D M 2001 *Phys. Rev. Lett.* **86** 870–3
[11] Ghosal A, Güçlü A D, Umrigar C J, Ullmo D and Baranger H U 2006 *Nat. Phys.* **2** 336–40
[12] Berry M V 1984 *Proc. R. Soc.* A **392** 45–57
[13] Trotzky S, Cheinet P, Folling S, Feld M, Schnorrberger U, Rey A M, Polkovnikov A, Demler E A, Lukin M D and Bloch I 2008 *Science* **319** 295–9
[14] Harowitz M, Shin D and Shumway J 2005 *J. Low Temp. Phys.* **140** 211–26
[15] Feynman R P 1972 *Statistical Mechanics* (Reading, MA: Addison-Wesley)
[16] Ceperley D M 1995 *Rev. Mod. Phys.* **67** 279–355
[17] Shumway J and Gilbert M 2008 Spin coupled quantum dots doi:10254/nanohub-r4963.1
[18] Harju A, Siljamäki S and Nieminen R M 2002 *Phys. Rev. Lett.* **88** 226804
[19] Schmidt K E and Lee M A 1995 *Phys. Rev.* E **51** 5495–8